Published in final edited form as:

Cancer Res. 2019 May 01; 79(9): 2415–2425. doi:10.1158/0008-5472.CAN-18-3177.

Inhibition of NF-κB–Dependent Signaling Enhances Sensitivity and Overcomes Resistance to BET Inhibition in Uveal Melanoma

Grazia Ambrosini[1], **Catherine Do**[2], **Benjamin Tycko**[2], **Ronald B. Realubit**[1], **Charles Karan**[1], **Elgilda Musi**[1], **Richard D. Carvajal**[1,3], **Vivian Chua**[4], **Andrew E. Aplin**[4], and **Gary K. Schwartz**[1,3]

[1]The Herbert Irving Comprehensive Cancer Center, Columbia University Medical Center, New York, New York.

[2]Division of Genetics & Epigenetics, Department of Biomedical Research, Hackensack-Meridian Health School of Medicine at Seton Hall University, Nutley, New Jersey.

[3]Division of Hematology/Oncology, Columbia University Medical Center, New York, New York.

[4]Cancer Biology and Sidney Kimmel Cancer Center, Thomas Jefferson University, Philadelphia, Pennsylvania.

Abstract

Bromodomain and extraterminal protein inhibitors (BETi) are epigenetic therapies aimed to target dysregulated gene expression in cancer cells. Despite early successes of BETi in a range of malignancies, the development of drug resistance may limit their clinical application. Here, we evaluated the mechanisms of BETi resistance in uveal melanoma, a disease with little treatment options, using two approaches: a high-throughput combinatorial drug screen with the clinical BET inhibitor PLX51107 and RNA sequencing of BETi-resistant cells. NF-kB inhibitors synergistically sensitized uveal melanoma cells to PLX51107 treatment.Furthermore, genes involved in NF-κB signaling were upregulated in BETi-resistant cells, and the transcription factor CEBPD contributed to the mechanism of resistance. These findings suggest that inhibitors of NF-κB signaling may improve the efficacy of BET inhibition in patients with advanced uveal melanoma.

Corresponding Author: Grazia Ambrosini, Columbia University Medical Center, The Herbert Irving Comprehensive Cancer Center, 1130 St. Nicholas Avenue, Room 207, New York, NY 10032., Phone: 212-851-4905; Fax: 212-851-4906; ga2391@cumc.columbia.edu.

Authors' Contributions

Conception and design: G. Ambrosini, G.K. Schwartz

Development of methodology: G. Ambrosini, B. Tycko, R.B. Realubit, C. Karan, G.K. Schwartz

Acquisition of data (provided animals, acquired and managed patients, provided facilities, etc.): B. Tycko, R.B. Realubit, C. Karan, E. Musi, G.K. Schwartz

Analysis and interpretation of data (e.g., statistical analysis, biostatistics, computational analysis): G. Ambrosini, C. Do, B. Tycko, R.B. Realubit, C. Karan, E. Musi, R.D. Carvajal, G.K. Schwartz

Writing, review, and/or revision of the manuscript: G. Ambrosini, B. Tycko, R.B. Realubit, C. Karan, R.D. Carvajal, A.E. Aplin, G.K. Schwartz

Administrative, technical, or material support (i.e., reporting or organizing data, constructing databases): R.B. Realubit, V. Chua, G.K. Schwartz

Introduction

Uveal melanoma is the most common intraocular malignancy in adults, with a very poor prognosis. The incidence of liver metastasis is 50% even after enucleation (1, 2), and the survival rates for patients with metastatic disease range from 4 to 15 months (3). Nearly 90% of uveal melanoma is characterized by oncogenic mutations in the G-protein alpha subunits q (GNAQ) and 11 (GNA11; refs. 4, 5). Gain of chromosome 8 and monosomy of chromosome 3 are poor prognostic markers (6), and amplification of Myc is present in about 40% of cases of uveal melanoma (7). Several treatments have been evaluated to date, including systemic chemotherapy, targeted agents for the MAPK pathway, immunotherapy, and liver-directed therapy. However, no treatment has been shown to improve overall survival (8, 9), and there is no standard therapy for the metastatic disease. Recent findings have highlighted the importance of epigenetic dysregulation, including CpG hypermethylation of candidate tumor suppressor genes and altered histone modifications in uveal melanoma tumorigenesis, progression, and metastasis (10). Chromatin regulators have become relevant targets for cancer therapy (11, 12), with examples including the bromodomain and extracellular domain (BET) proteins BRD2, BRD3, BRD4, and BRDT, which play a central role in transcription and cell growth. BRD4 is known to recruit the transcriptional elongation factor complex (PTEFb) to chromatin and activate RNA polymerase II-dependent transcription. BET inhibition by small molecules downregulates MYC transcription, followed by genome-wide downregulation of Myc-dependent target genes (13). Several small-molecule inhibitors specifically targeting the bromodo-mains of BET proteins have been developed that display promising anticancer activity via selective inhibition of promoter activity of genes with oncogenic roles in hematologic (14) and solid tumors (15). We previously reported that JQ1, a BRD4 inhibitor, induced cell-cycle arrest in uveal melanoma cell lines, and it had proapoptotic effects in cells with GNAQ/11 mutations, irrespective of MYC status (16). Transcriptional microarray analysis revealed that GNAQ/11 mutant cells are highly dependent on BRD4 activity compared with cells without the mutations, and we identified two genes, Bcl-xL and Rad51, as important targets of JQ1 in GNAQ/11-mutant cells.

Although BET inhibitors are currently being evaluated in clinical trials across a range of malignancies, the molecular and cellular mechanisms responsible for resistance to this class of drugs are starting to emerge. For example, evidence of primary and acquired resistance to BETi has been described in myeloid leukemia through activation of WNT/b-catenin signaling components (17, 18). In prostate cancer, intrinsic BETi resistance was reported to be mediated by BET protein stabilization and AKT-mTORC1 activation (19), whereas TRIM33 was identified as a factor promoting sensitivity to BETi through Myc and TGFβ in colorectal cancer (20). Because these mechanisms of BETi sensitivity and resistance seem to be tumor type-dependent, exploring this phenomenon in uveal melanoma may lead to novel and more successful treatments. The BETi PLX51107 is currently being evaluated in a clinical trial () for the treatment of solid tumors, including uveal melanoma. Here, we report high-throughput drug screening and RNA sequencing analysis of uveal melanoma cells to uncover the mechanisms of resistance to BETi, with the goal of developing combination therapies that overcome drug resistance in this treatment-refractory disease.

Materials and Methods

Cell lines and reagents

Omm1.3 and Omm1 cell lines were kindly provided by Dr B. Bastian, University of California, San Francisco, CA. The cell line 92.1 was provided by Dr W. Harbour, Washington University, St. Louis, MO. The cell line UM004 was provided by Dr. Takami Sato, Thomas Jefferson University, Philadelphia, PA. All cell lines were sequenced for the presence of activating mutations in codons 209 of Gnaq and Gna11. Mewo cells were purchased from ATCC. The cells were cultured in RPMI medium supplemented with 10% FBS, 100 U/mL penicillin and 100 mg/mL streptomycin, and maintained at 37°C in 5%CO_2. The resistant cell lines were derived from the corresponding parental cell lines after at least 6 weeks of exposure to escalating doses of PLX51107. The surviving cells were then routinely grown in 0.2 to 0.5 μmmol/L PLX51107. PLX51107 and PLX8573 were from Plexxikon, Inc. JQ1 and QNZ (EVP4593) were from Selleck Chemicals.

High-throughput screening

A large-scale drug combination experiment was carried out using a library of 1,280 compounds (Tocris), which was tested in 4 concentrations (5, 1, 0.2, and 0.04 μmmol/L) versus 4 concentrations of PLX51107 (0.17, 0.08, 0.04, and 0.02 μmmol/L). This resulted in the generation of 20,480 combinations in triplicate (61,440 total). We utilized an Echo 550 acoustic dispensing system to dispense the compounds in the drug combination matrices. Each individual combination was run on a single assay plate, and an additional plate was run to provide the effect of the library compound in the absence of PLX51107. Each assay plate also contained PLX51107 treatments in the absence of additional compounds, a positive control (Thimerosal at 20 μmmol/L) and a negative control (DMSO). CellTiterGlo (Promega) was used to assess the viability of each well through quantification of ATP levels. Using the individual drug treatment and the corresponding drug combination response, an excess over Bliss for each combination was derived (21). Combinations with high bliss score were brought forward for further testing and run in 10 × 20 concentration matrixes.

Cell viability assays

Cell viability was measured after 3 days of treatments in 96 well plates using the Cell Counting Kit 8 (CCK8) from Dojindo Molecular Technologies, and expressed as a percentage of untreated cells. Cell-cycle analysis was performed by flow cytometry after staining the cells with 5 μmg/mL propidium iodide in the presence of 50 μmg/mL RNase A. The data were analyzed using FlowJo software. Apoptosis was measured using a chromatin condensation and membrane permeability apoptosis assay (YO-PRO-1, Life Technologies). Fluorescent cells were analyzed on Cellometer K2 (Nexcelom Bioscience) with De Novo software.

RNA sequencing and gene set enrichment analysis

The cells were treated in triplicate with medium containing 0.2% DMSO or 0.5 μmmol/L PLX51107 for 24 hours. Total RNA was extracted using the RNeasy Mini Kit (Qiagen) and RNA integrity was confirmed on a Bio Analyzer (Agilent Technologies). Poly-A pull-down

was used to enrich for mRNAs, and libraries were prepared using the Illumina TruSeq RNA Kit. Libraries were pooled and sequenced on an Illumina HiSeq2000 machine with 100-bp single-end reads. RTA (Illumina) was used for base calling and bcl2fastq (version 1.8.4) for converting BCL to FASTQ format, coupled with adaptor trimming. The reads were mapped to the human reference genome (NCBI/build37.2) using Tophat (22) with 4 mismatches and 10 maximum multiple hits. The relative expression level of genes was estimate by FPKM (fragments per kilobase of transcript per million mapped reads) using Cufflinks (23) with default settings. For each condition, we averaged the FPKM across 3 technical replicates. We excluded from subsequent analysis one locus, *HBB*, for which the FPKM value was aberrant in one of the replicate and reflected genomic DNA contamination. Correlations between technical replicates were estimated by R^2 calculated by linear regression. Candidate genes were defined as genes with at least 1.5-fold change and 1 FPKM in absolute difference in at least 2 cell lines. Data are deposited at GEO no. GSE124059. Gene lists of interest were analyzed for the enrichment of biological pathways using hypergeometric tests with Benjamini–Hochberg multiple testing correction (FDR). To test for this enrichment, we downloaded hallmark gene sets, which aggregate several MSigDB gene sets from GSEA-Broad Institute database (www.broadinstitute.org/gsea). All statistical analyses were carried out using R and Stata statistical software v13 (Stata Corp).

Immunoblotting

Cells were lysed in RIPA buffer (Cell Signaling Technology) supplemented with protease inhibitor cocktail tablets (Roche Diagnostics). Total protein concentration of the lysates was measured by BCA assay (Bio-Rad), and equal amounts of protein were loaded on 4% to 12% PAGE gels (Life Technologies). PVDF membranes were blocked with 5% nonfat dried milk in TBS buffer and probed with antibody for p65, p-p65, p50, IkBα, c-Myc, PARP, REL, RELB, tubulin (Cell Signaling Technology), CEBPD, and SOD2 (Santa Cruz Biotechnology). Signals from secondary antibodies were detected using ECL (Pierce) and auto-radiography films (Thermo Fisher Scientific). Antibodies for IHC (p-p65 and CEBPD) were from Abcam.

siRNA and plasmid transfections

Two nontargeting and specific siRNA sets against p65, IkBα, REL, RELB, CEBPD, and SOD2 were purchased from Santa Cruz Biotechnology, Dharmacon, or Thermo Fisher Scientific. Sequences are listed in Supplementary Table S1. They were transfected in cells using Lipofectamine RNAiMAX reagent (Life Technologies). CEBPD cDNA construct was from GenScript, and it was transfected in cells using Fugene 6 (Promega) following the manufacturer's instructions. NF-κB-Luciferase reporter gene vector and reagents were from Promega.

qRT-PCR

Total RNA was reverse-transcribed using the SuperScript IV First Strand System (Life Technologies). The resultant cDNA was used in qPCR reactions using 7500 Real Time PCR System (Applied Biosystems) with predesigned TaqMan Gene expression assays for REL, RELB, CEBPD, SOD2, and GAPDH genes (Life Technologies). The relative expression of each gene was calculated by the $\Delta\Delta C_t$ method in triplicates and normalized with GAPDH.

Each experiment was performed three times in triplicates. Values (folds) are relative to mRNA levels of 92.1 untreated cells set at 1.

Animal studies

Athymic nu/nu mice were purchased from Charles River Laboratories, and used when they were 8 weeks old. R-Omm1.3 cells were inoculated subcutaneously into the right flanks of four mice. When tumors reached a volume of approximately 1,000 mm^3 diameter, they were dissected and implanted in mice before the experiment. When these tumors reached an average of 270 mm^3 diameter, the mice were administered (7/group) with vehicle or PLX51107 20 mg/kg orally PTL 10 mg/kg i.p. and the combination of the two drugs three times a week. The treatment duration was 5 weeks and the tumor size and body weights were measured twice a week. Two animals in each cohort were sacrificed and the resected tumors were snap frozen for Western blot analysis. Experiments were carried out under an Institutional Animal Care and Use Committee–approved protocol, and institutional guidelines for the proper and humane use of animals were followed. Statistical significance was determined by two-sample Student *t* tests.

Patient tumor samples

Biopsies were collected from liver metastasis of patients enrolled in the PLX51107 clinical trial () following written informed consent under an IRB-approved protocol (#02.9014R) and confirmed to be metastatic uveal melanoma. The tissue samples were fixed in buffered formalin (1:10) for 24 hours, then embedded in paraffin, and sections were stained with p-p65 and CEBPD antibodies by IHC.

Results

Identification of compounds that synergize with PLX51107

Uveal melanoma cells have shown sensitivity to the clinical BET inhibitor PLX51107 *in vitro* and in xenograft mouse models (Supplementary Fig. S1A and S1B), consistent with our previous findings using the BRD4 inhibitor JQ1 (16). To increase the effectiveness of BET inhibition in uveal melanoma, we explored combinatorial treatments utilizing a high-throughput drug screening library of 1,280 FDA-approved and experimental compounds in combination with PLX51107. The uveal melanoma cell line 92.1 was treated in 4 × 4 matrix of PLX51107 either alone or in combination with each compound at concentrations ranging from 0.04 to 5 μmmol/L, and evaluated following 72 hours of drug exposure. Four hits were selected in the primary screening based on Bliss synergy score (24). Notably, two of four compounds, parthenolide (PTL) and ammonium pyrrolidine dithiocarbamate (PDTC) are known NF-κB inhibitors (25–27). They were subjected to secondary screening in a 10 × 20 matrix to confirm their activity, and we found that PTL had the most significant Bliss score for synergy in combination with PLX51107 (Fig. 1A). Synergy was also confirmed with the Chou–Talalay method (28), with resulting combination index < 1 (Fig. 1B). To confirm inhibition of NF-κB signaling by PTL we performed NF-κB reporter gene assays, where the relative luciferase activity was inhibited by PTL alone and in combination with PLX51107 in 92.1 cells (Fig. 1C) and Omm1.3 cells (Supplementary Fig. S2A). PTL also inhibited the phosphorylation of the NF-κB subunit p65 in 92.1 (Fig. 1D) and Omm1.3 cells

(Supplementary Fig. S2B). Furthermore, the combination PLX51107+ PTL suppressed the expression of the subunit p50, inducedþthe NF-κB inhibitor IkBα, and increased PARP cleavage in both cell lines. Apoptotic cells increased 2.5-fold with the combination treatment compared with single agents in 92.1 (Fig. 1E) and Omm1.3 cells (Supplementary Fig. S2C). To confirm the specificity of NF-κB inhibition, we silenced p65 and IkBα with two independent siRNAs in uveal melanoma cells (Fig. 1F; Supplementary Fig. S2D). After p65 depletion, we found a decrease in NF-κB activity (Fig. 1G) and cell viability (Fig. 1H), reproducing PTL effects. In contrast, the silencing of IkBα increased NF-κB activity (Fig. 1G) and rendered the cells less sensitive to PLX51107 (Fig. 1H; Supplementary Fig. S2E). We also analyzed the effects of the second NF-κB inhibitor, PDTC, obtaining similar combination effects with PLX51107 (Supplementary Fig. S3A–S3C). These results indicate that the inhibition of NF-κB signaling has synergistic antiproliferative activities with the BET inhibitor PLX51107 in uveal melanoma cells.

Uveal melanoma cells acquire resistance to PLX51107

Using another approach, we developed BETi-resistant uveal melanoma cell lines to explore mechanisms of acquired resistance to BET inhibitors. Uveal melanoma cell lines were chronically exposed to increasing doses of PLX51107 (0.05—2 μmmol/L) for at least 6 weeks. Four independent uveal melanoma cell lines were established, which showed resistance to BETi treatments (Fig. 2A), with IC_{50} that were 5- to 10-fold higher than their parental cell lines (Fig. 2B). The cells also showed cross-resistance to the BRD4 inhibitor JQ1 (Supplementary Fig. S4A) and another potent BET inhibitor, PLX72583 (Supplementary Fig. S4B).

We further characterized the resistant cells, which did not show changes in cell size (Supplementary Fig. S4C); instead, they grew at slower rates compared with their parental cell lines (Supplementary Fig. S4D). We next analyzed cell-cycle progression after PLX51107 treatment for 48 hours. In the parental cells, we found an arrest in G_1-phase and an increase in the sub-G_1 population (Fig. 2C). In contrast, the resistant cells remained mostly unchanged after the treatment. Moreover, PLX51107 induced PARP cleavage in the parental cells only (Fig. 2D). Interestingly, the BRD4 target c-Myc was downregulated by PLX51107 in both parental and resistant cells (Fig. 2D), suggesting that the drug is still blocking BET proteins, but it fails to induce cell-cycle arrest and apoptosis in the resistant cells.

To search for mechanisms driving resistance, we analyzed the transcriptomes of four parental and four BETi-resistant uveal melanoma cell lines by RNA sequencing. For comparison, we analyzed parental and resistant cutaneous melanoma cells (Mewo). The cells were treated with DMSO or 0.5 μmmol/L PLX51107 for 24 hours and the differential analysis of genes was performed using FPKM calculated by Cufflink. We observed high correlations between technical replicates (R2 ranging from 0.91 to 0.999), but to decrease the risk of false-positive biological findings, we required reproducible expression changes in multiple cell lines, instead of significant P value based on technical replicates. In a first analysis, we found that many genes regulated by acute drug exposure in the sensitive uveal melanoma cells were no longer induced or repressed after drug resistance had developed,

suggesting the acquisition of stable epigenetic changes in BETi target genes. Therefore, we searched for differentially expressed (DE) genes in the BETi-resistant cells at baseline versus BETi-sensitive cells. Candidate genes were defined with at least 1.5-fold change and 1 FPKM in absolute difference in at least 2 cell lines. Using this approach, we found 799 overexpressed and 1,019 underex-pressed genes in the BETi-resistant cells (Fig. 3A).

Next, we searched for regulatory pathways driving resistance and performed gene set enrichment analysis (GSEA) on these DE genes, which pointed to alterations in major signaling pathways, including NF-κB signaling, the epithelial–mesenchymal transition (EMT), estrogen response, hypoxia, and STAT5 signaling (Fig. 3B). Focusing on specific genes in these pathways, we found that genes involved in NF-κB signaling (REL, RELB, CEBPD, SOD2), and in the EMT (CD44, SNAI2, GADD45B) were upregulated in the resistant cell lines, while underex-pressed genes were mostly involved in hypoxia (IGFBP3, CDKN1C) and STAT5 signaling (SOCS1 and SLC2A3). In contrast, the cutaneous melanoma Mewo cells did not show significant changes in the expression of these genes (Supplementary Fig. S5A). There were no enriched pathways for over-expressed genes in the resistant Mewo cells, as most of the genes were downregulated, including those of the NF-κB signaling pathway (Supplementary Fig. S5B). This finding is in accordance with previous reports showing that BET inhibition suppressed NF-κB genes in cutaneous melanoma (29). In fact, the combination with PTL did not increase the sensitivity to PLX51107 (Supplementary Fig. S5C). Furthermore, there was very little overlap of genes between uveal melanoma and Mewo cells (Venn diagram, Supplementary Fig. S5D), suggesting that the gene sets found in the BETi-resistant uveal melanoma cells are unique for this cell type.

NF-κB signaling mediates acquired resistance to BET inhibition

On the basis of the GSEA analysis, we first sought to confirm the induction of several genes involved in the NF-κB signaling (REL, RELB, CEBPD, SOD2) in all the resistant cell lines by qPCR (Fig. 3C) and immunoblotting (Fig. 3D). Both assays showed higher expression of these genes at the mRNA and protein level in the resistant cells compared with their parental counterpart. Furthermore, NF-κB activity was increased in the resistant cells compared with parental (Fig. 4A), and it could be inhibited by PTL. To test whether NF-κB inhibition could also reverse secondary BETi resistance, we treated the resistant cells with PTL or another known NF-κB inhibitor, QNZ (EVP4593), and found that both combinations were synergistic (Fig. 4B; Supplementary Fig. S6A), and induced significant apoptosis in the resistant cells R-92.1 and R-Omm1.3 (Fig. 4C; Supplementary Figs. S6B, S7A, and S7B). Next, we tested the expression of the above-mentioned genes in parental and resistant cells after treatments. The combination PLX51107+PTL decreased p-p65 and p50, while it induced IkBα and PARP cleavage in both parental and resistant cells (Fig. 4D and E). In addition, CEBPD was downregulated by the combination in the resistant cell lines, while PLX51107 alone was sufficient to suppress it in the parental cells. RELB, REL, and SOD2 expression did not significantly change after the treatments. These data suggest that NF-κB inhibitors synergize with PLX51107 in both parental and resistant cells by decreasing the expression of NF-κB signaling molecules and inducing apoptosis.

We next utilized a mouse xenograft model of BETi-resistant uveal melanoma cells to test the effects of the combination PLX51107+PTL *in vivo*. Tumors developed from R-Omm1.3 cells were passaged in mice until they reached an average volume of 270 mm^3. The mice were treated with vehicle, 20 mg/kg orally PLX51107, 10 mg/kg i.p. PTL, and the combination of the two drugs. The combination of PLX51107 + PTL could significantly inhibit tumor growth in a dose-dependent manner compared with vehicle or PLX51107 single agent (Fig. 5A), suggesting that PTL could reverse resistance to PLX51107 *in vivo*. These treatments did not cause reduced body weight of the host mice (Fig. 5B) or other side effects. Western blot analysis of tumor specimens from two mice in each group showed downregulation of target genes (i.e., p-p65, p50, CEBPD) especially with the combination therapy (Fig. 5C).

CEBPD contributes to NF-κB signaling and BETi resistance

To determine whether any particular gene was involved in BETi resistance, we silenced CEBPD, REL, RELB, and SOD2 with two independent siRNAs for each gene (Fig. 6A). NF-κB activity was measured in the siRNA-depleted cells, showing decreased activity especially after CEBPD depletion (Fig. 6B). This is in accordance with previous studies, where CEBPD engages in cross-talk and synergizes with the NF-κB pathway (30, 31). Furthermore, the depletion of each gene in the resistant cells slightly decreased cell viability after treatment with PLX51107 (Fig. 6C), while the suppression of CEBPD induced a significant reversal of resistance. Next, we assessed whether the exogenous expression of CEBPD could protect the cells from the combination treatment. Although CEBPD synergizes with NF-κB subunits by direct binding (31), we also found that in the presence of CEBPD overexpression (Fig. 6D), there was residual p-p65 after the combination treatment. Indeed, CEBPD over- expression increased NF-κB activity (Fig. 6E) and significantly rescued the cells from the combination treatment, compared with vector control (Fig. 6F).

Finally, we sought to determine the expression levels of p-p65 and CEBPD in tumor biopsy samples from patients enrolled in the PLX51107 clinical trial. A total of 36 patients with advanced solid tumors were treated on this study, including 11 patients with uveal melanoma. Although there were no responses, 8 patients achieved stable disease (SD), including 2 with uveal melanoma. Specimens at baseline (pre-treatment) and on PLX51107 (2 weeks posttreatment) from two representative patients with uveal melanoma were analyzed by IHC. The expression of p-p65 did not change after treatment with PLX51107 (Supplementary Fig. S7C). However, the intensity of CEBPD staining was suppressed in patient UM-1, who achieved prolonged stable disease lasting over 1 year (Fig. 6G). Patient UM-2 showed no significant changes in CEBPD expression and experienced disease progression, suggesting that these patients, especially patient UM-2, may benefit from a combination with a NF-κB inhibitor.

Altogether, these results suggest that NF-κB signaling mediates resistance to BET inhibition in uveal melanoma cells, and CEBPD, a transcription factor that synergizes with the NF-κB pathway, contributes to the acquired resistance to PLX51107.

Discussion

In recent years, BET inhibitors have shown efficacy in preclinical studies in uveal melanoma (16), in cutaneous melanoma (32) and other solid tumors (15). However, results from the first clinical trials show limited single-agent activity and the development of drug resistance may limit their clinical application (12). To increase the efficacy of BET inhibition in uveal melanoma, we have explored combinatorial strategies using a large library of compounds in combination with the clinical BET inhibitor PLX51107. We found synergistic activities of two NF-κB inhibitors, PTL and PDTC, in combination with PLX51107. PTL, which had the most significant synergy score, is a sesquiterpene lactone found in feverfew and it was reported to exert toxicity against a wide range of cancer cells as single agent and in combination with other anticancer drugs (33, 34).

We have also analyzed the transcriptome of sensitive and BETi-resistant uveal melanoma cell lines. RNA sequencing analysis revealed that several genes involved in NF-κB signaling were overexpressed in cells with acquired resistance to PLX51107. One of these genes, the transcription factor CEBPD, contributed to BETi secondary resistance, and the combination with NF-κB inhibitors could restore sensitivity to BET inhibition in uveal melanoma resistant cells and mouse models. Thus, both strategies revealed that inhibition of NF-κB signaling enhances sensitivity to BET inhibition and can reverse resistance to PLX51107 in uveal melanoma cells.

The NF-κB signaling pathway is a key coordinator of immunity and inflammation, a regulator of tumor initiation and progression, and it can also function as a resistance factor against treatments such as chemotherapy (35, 36), targeted therapy (37) and immune-response (38). The role of NF-κB in the resistance to BETi appears to be cell type-dependent. In fact, this pathway was reported to be downregulated in BETi-resistant leukemia cells (17), and it was also suppressed by BRD4 inhibitors in melanoma (29) and lung carcinoma (39). On the contrary, we showed that NF-κB signaling was active in uveal melanoma cells after BET inhibition and it was exacerbated during the acquisition of secondary resistance with the upregulation of several NF-κB dependent genes. The NF-κB family members can form up to 15 different dimers with other members of the family, and their activity is regulated mostly by posttranscriptional modifications and subcellular localization. However, the molecular or pharmacologic suppression of CEBPD was sufficient to resensitize the resistant cells to PLX51107. This protein belongs to the CCAAT/enhancer-binding protein family, functioning as a transcription factor in many biological processes, including cell differentiation, proliferation, cell death, and inflammation (40, 41). All members of this family (CEBPA/B/D) engage in cross-talk with NF-κB (30, 31). CEBPD can amplify NF-κB–mediated transcription, resulting in the synergistic stimulation of promoters with C/EBP-binding sites (41), including promoters of immune or acute-phase responding genes, such as IL8 (42). In the resistant cells, we found upregulation of the proinflammatory cytokine IL17D, which also activates NF-κB (43). Inhibiting these responses with NF-κB antagonists may overcome a tumor-promoting inflammatory microenvironment, in which uveal melanoma cells actively participate (44). CEBPD has been also implicated in the acquisition of resistance to drugs such as cisplatin and methoxyestradiol through the expression of SOD1 (45) and SOD2 (46), respectively. SOD2

was indeed upregulated in uveal melanoma–resistant cells, where it may play a role in protecting the cells from oxidative stress (47). We also analyzed the expression of CEBPD in liver biopsies of patients with uveal melanoma treated with PLX51107. These results would suggest that downregulating CEBPD with a NF-kB inhibitor could improve the efficacy of BET inhibition in patients with uveal melanoma. However, further studies are required to evaluate NF-κB and CEBPD expression in tissue samples from patients treated with BET inhibitors.

Numerous NF-κB inhibitors have been developed that may be used to block this signaling pathway (48). A number of protea-some inhibitors can also act as NF-κB inhibitors and are in clinical development. The most studied is bortezomib, the first NF-κB blocking drug approved by the FDA (49). Other examples are etanercept, an inhibitor commonly used for rheumatoid arthritis that has been recently shown to inhibit the metastatic potential of ovarian cancer cells (50), and selinexor, an inhibitor of NF-κB transport and activity through the inhibition of the nuclear export protein XPO1 (51).

In conclusion, this study extends our understanding of the molecular mechanisms underlying BETi resistance in uveal melanoma, and it could lead to more effective treatments against this disease.

Supplementary Material

Refer to Web version on PubMed Central for supplementary material.

Acknowledgments

The work was supported by the Melanoma Research Alliance (MRA) #402803 and NIH R01 160495. We thank Plexxikon Inc. for providing PLX51107. We also thank the Columbia University Pathology core and the Confocal Microscopy facility for assistance with IHC.

The costs of publication of this article were defrayed in part by the payment of page charges. This article must therefore be hereby marked *advertisement* in accordance with 18 U.S.C. Section 1734 solely to indicate this fact.

Disclosure of Potential Conflicts of Interest

R.D. Carvajal is a consultant/advisory board member for Array, BMS, Pure-Tech Health, Sanofi Genzyme, Sorrento Therapeutics, Aura Biosciences, Chimeron, Rgenix, Castle Biosciences, Compugen, Foundation Medicine, Immunocore, I-Mab, Incyte, Merck, and Roche/Genentech. A.E. Aplin reports receiving a commercial research grant from Pfizer and is a consultant/advisory board member for SpringWorks Therapeutics and Fortress Biotech. No potential conflicts of interest were disclosed by the other authors.

References

1. Diener-West M, Reynolds SM, Agugliaro DJ, Caldwell R, Cumming K, Earle JD, et al. Development of metastatic disease after enrollment in the COMS trials for treatment of choroidal melanoma: Collaborative Ocular Melanoma Study Group Report No. 26. Arch Ophthalmol 2005;123: 1639–43. [PubMed: 16344433]
2. Kuk D, Shoushtari AN, Barker CA, Panageas KS, Munhoz RR, Momtaz P, et al. Prognosis of mucosal, uveal, acral, nonacral cutaneous, and unknown primary melanoma from the time of first metastasis. Oncologist 2016;21: 848–54. [PubMed: 27286787]
3. Kujala E, Makitie T, Kivela T. Very long-term prognosis of patients with malignant uveal melanoma. Invest Ophthalmol Vis Sci 2003;44: 4651–9. [PubMed: 14578381]

4. Van Raamsdonk CD, Bezrookove V, Green G, Bauer J, Gaugler L, O'Brien JM, et al. Frequent somatic mutations of GNAQ in uveal melanoma and blue naevi. Nature 2009;457:599–602. [PubMed: 19078957]
5. Van Raamsdonk CD, Griewank KG, Crosby MB, Garrido MC, Vemula S, Wiesner T, et al. Mutations in GNA11 in uveal melanoma. N Engl J Med 2010;363:2191–9. [PubMed: 21083380]
6. van den Bosch T, van Beek JG, Vaarwater J, Verdijk RM, Naus NC, Paridaens D, et al. Higher percentage of FISH-determined monosomy 3 and 8q amplification in uveal melanoma cells relate to poor patient prognosis. Invest Ophthalmol Vis Sci 2012;53:2668–74. [PubMed: 22427574]
7. Parrella P, Caballero OL, Sidransky D, Merbs SL. Detection of c-myc amplification in uveal melanoma by fluorescent in situ hybridization. Invest Ophthalmol Vis Sci 2001;42:1679–84. [PubMed: 11431428]
8. Carvajal RD. Update on the treatment of uveal melanoma. Clin Adv Hematol Oncol 2016;14:768–70. [PubMed: 27930627]
9. Komatsubara KM, Manson DK, Carvajal RD. Selumetinib for the treatment of metastatic uveal melanoma: past and future perspectives. Future Oncol 2016;12:1331–44. [PubMed: 27044592]
10. Li Y, Jia R, Ge S. Role of epigenetics in uveal melanoma. Int J Biol Sci 2017; 13:426–33. [PubMed: 28529451]
11. Dawson MA, Kouzarides T, Huntly BJ. Targeting epigenetic readers in cancer. N Engl J Med 2012;367:647–57. [PubMed: 22894577]
12. Stathis A, Bertoni F. BET proteins as targets for anticancer treatment. Cancer Discov 2018;8:24–36. [PubMed: 29263030]
13. Delmore JE, Issa GC, Lemieux ME, Rahl PB, Shi J, Jacobs HM, et al. BET bromodomain inhibition as a therapeutic strategy to target c-Myc. Cell 2011;146:904–17. [PubMed: 21889194]
14. Dawson MA, Prinjha RK, Dittmann A, Giotopoulos G, Bantscheff M, Chan WI, et al. Inhibition of BET recruitment to chromatin as an effective treatment for MLL-fusion leukaemia. Nature 2011;478:529–33. [PubMed: 21964340]
15. Sahai V, Redig AJ, Collier KA, Eckerdt FD, Munshi HG. Targeting BET bromodomain proteins in solid tumors. Oncotarget 2016;7: 53997–4009. [PubMed: 27283767]
16. Ambrosini G, Sawle AD, Musi E, Schwartz GK. BRD4-targeted therapy induces Myc-independent cytotoxicity in Gnaq/11-mutatant uveal melanoma cells. Oncotarget 2015;6:33397–409. [PubMed: 26397223]
17. Fong CY, Gilan O, Lam EY, Rubin AF, Ftouni S, Tyler D, et al. BET inhibitor resistance emerges from leukaemia stem cells. Nature 2015; 525:538–42. [PubMed: 26367796]
18. Rathert P, Roth M, Neumann T, Muerdter F, Roe JS, Muhar M, et al. Transcriptional plasticity promotes primary and acquired resistance to BET inhibition. Nature 2015;525:543–7. [PubMed: 26367798]
19. Zhang P, Wang D, Zhao Y, Ren S, Gao K, Ye Z, et al. Intrinsic BET inhibitor resistance in SPOP-mutated prostate cancer is mediated by BET protein stabilization and AKT-mTORC1 activation. Nat Med 2017; 23:1055–62. [PubMed: 28805822]
20. Shi X, Mihaylova VT, Kuruvilla L, Chen F, Viviano S, Baldassarre M, et al. Loss of TRIM33 causes resistance to BET bromodomain inhibitors through MYC- and TGF-beta-dependent mechanisms. Proc Natl Acad Sci U S A 2016;113:E4558–66. [PubMed: 27432991]
21. Zhao W, Sachsenmeier K, Zhang L, Sult E, Hollingsworth RE, Yang H. A new Bliss independence model to analyze drug combination data. J Biomol Screen 2014;19:817–21. [PubMed: 24492921]
22. Trapnell C, Pachter L, Salzberg SL. TopHat: discovering splice junctions with RNA-Seq. Bioinformatics 2009;25:1105–11. [PubMed: 19289445]
23. Trapnell C, Williams BA, Pertea G, Mortazavi A, Kwan G, van Baren MJ, et al. Transcript assembly and quantification by RNA-Seq reveals unan notated transcripts and isoform switching during cell differentiation. Nat Biotechnol 2010;28:511–5. [PubMed: 20436464]
24. Borisy AA, Elliott PJ, Hurst NW, Lee MS, Lehar J, Price ER, et al. Systematic discovery of multicomponent therapeutics. Proc Natl Acad Sci U S A 2003; 100:7977–82. [PubMed: 12799470]

25. Kwok BH, Koh B, Ndubuisi MI, Elofsson M, Crews CM. The anti-inflammatory natural product parthenolide from the medicinal herb Feverfew directly binds to and inhibits IkappaB kinase. Chem Biol 2001;8:759–66. [PubMed: 11514225]
26. Kim SL, Kim SH, Park YR, Liu YC, Kim EM, Jeong HJ, et al. Combined Parthenolide and balsalazide have enhanced antitumor efficacy through blockade of NF-kappaB activation. Mol Cancer Res 2017;15:141–51. [PubMed: 28108625]
27. Li S, Zhong S, Zeng K, Luo Y, Zhang F, Sun X, et al. Blockade of NF-kappaB by pyrrolidine dithiocarbamate attenuates myocardial inflammatory response and ventricular dysfunction following coronary microembolization induced by homologous microthrombi in rats. Basic Res Cardiol 2010; 105:139–50. [PubMed: 19823892]
28. Chou TC. Drug combination studies and their synergy quantification using the Chou-Talalay method. Cancer Res 2010;70:440–6. [PubMed: 20068163]
29. Gallagher SJ, Mijatov B, Gunatilake D, Gowrishankar K, Tiffen J, James W, et al. Control of NF-κB activity in human melanoma by bromodomain and extra-terminal protein inhibitor I-BET151. Pigment Cell Melanoma Res 2014;27:1126–37. [PubMed: 24924589]
30. Xia C, Cheshire JK, Patel H, Woo P. Cross-talk between transcription factors NF-kappa B and C/EBP in the transcriptional regulation of genes. Int J Biochem Cell Biol 1997;29:1525–39. [PubMed: 9570146]
31. Stein B, Cogswell PC, Baldwin AS Jr. Functional and physical associations between NF-kappa B and C/EBP family members: a Rel domain-bZIP interaction. Mol Cell Biol 1993;13:3964–74. [PubMed: 8321203]
32. Segura MF, Fontanals-Cirera B, Gaziel-Sovran A, Guijarro MV, Hanni-ford D, Zhang G, et al. BRD4 sustains melanoma proliferation and represents a new target for epigenetic therapy. Cancer Res 2013;73: 6264–76. [PubMed: 23950209]
33. Dey S SM, Giri B. Anti-inflammatory and anti-tumor activities of parthenolide: an update. J Chem Biol Ther 2016;1:107–13.
34. Wyrebska A, Gach K, Janecka A. Combined effect of parthenolide and various anti-cancer drugs or anticancer candidate substances on malignant cells in vitro and in vivo. Mini Rev Med Chem 2014;14: 222–8. [PubMed: 24552263]
35. Seubwai W, Vaeteewoottacharn K, Kraiklang R, Umezawa K, Okada S, Wongkham S. Inhibition of NF-kappaB activity enhances sensitivity to anticancer drugs in cholangiocarcinoma cells. Oncol Res 2016;23: 21–8.
36. Li Q, Yang G, Feng M, Zheng S, Cao Z, Qiu J, et al. NF-kappaB in pancreatic cancer: its key role in chemoresistance. Cancer Lett 2018;421: 127–34. [PubMed: 29432846]
37. Darvishi B, Farahmand L, Eslami SZ, Majidzadeh AK. NF-kappaB as the main node of resistance to receptor tyrosine kinase inhibitors in triple-negative breast cancer. Tumour Biol 2017;39:1–10.
38. Grinberg-Bleyer Y, Oh H, Desrichard A, Bhatt DM, Caron R, Chan TA, et al. NF-kappaB c-Rel is crucial for the regulatory T cell immune checkpoint in cancer. Cell 2017;170:1096–108. [PubMed: 28886380]
39. Zou Z, Huang B, Wu X, Zhang H, Qi J, Bradner J, et al. Brd4 maintains constitutively active NF-kappaB in cancer cells by binding to acetylated RelA. Oncogene 2014;33:2395–404. [PubMed: 23686307]
40. Balamurugan K, Sterneck E.The many faces of C/EBPdelta and their relevance for inflammation and cancer. Int J Biol Sci 2013;9:917–33. [PubMed: 24155666]
41. Ko CY, Chang WC, Wang JM. Biological roles of CCAAT/Enhancer-binding protein delta during inflammation. J Biomed Sci 2015;22:6. [PubMed: 25591788]
42. Stein B, Baldwin AS Jr. Distinct mechanisms for regulation of the inter-leukin-8 gene involve synergism and cooperativity between C/EBP and NF-kappa B. Mol Cell Biol 1993;13:7191–8. [PubMed: 8413306]
43. Shalom-Barak T, Quach J, Lotz M. Interleukin-17-induced gene expression in articular chondrocytes is associated with activation of mitogen-activated protein kinases and NF-kappaB. J Biol Chem 1998;273: 27467–73. [PubMed: 9765276]

44. Jehs T, Faber C, Juel HB, Bronkhorst IH, Jager MJ, Nissen MH. Inflammation-induced chemokine expression in uveal melanoma cell lines stimulates monocyte chemotaxis. Invest Ophthalmol Vis Sci 2014;55: 5169–75. [PubMed: 25074768]
45. Hour TC, Lai YL, Kuan CI, Chou CK, Wang JM, Tu HY, et al. Transcriptional up-regulation of SOD1 by CEBPD: a potential target for cisplatin resistant human urothelial carcinoma cells. Biochem Pharmacol 2010; 80:325–34. [PubMed: 20385105]
46. Zhou J, Du Y. Acquisition of resistance of pancreatic cancer cells to 2-methoxyestradiol is associated with the upregulation of manganese superoxide dismutase. Mol Cancer Res 2012;10:768–77. [PubMed: 22547077]
47. Fukui M, Zhu BT. Mitochondrial superoxide dismutase SOD2, but not cytosolic SOD1, plays a critical role in protection against glutamate-induced oxidative stress and cell death in HT22 neuronal cells. Free Radic Biol Med 2010;48:821–30. [PubMed: 20060889]
48. Gupta SC, Sundaram C, Reuter S, Aggarwal BB. Inhibiting NF-kappaB activation by small molecules as a therapeutic strategy. Biochim Biophys Acta 2010;1799:775–87. [PubMed: 20493977]
49. Dingli D, Rajkumar SV. Emerging therapies for multiple myeloma. Oncology (Williston Park) 2009;23:407–15. [PubMed: 19476273]
50. Cho U, Kim B, Kim S, Han Y, Song YS. Pro-inflammatory M1 macrophage enhances metastatic potential of ovarian cancer cells through NF-kappaB activation. Mol Carcinog 2018;57:235–42. [PubMed: 29024042]
51. Nair JS, Musi E, Schwartz GK. Selinexor (KPT-330) induces tumor suppression through nuclear sequestration of IkappaB and downregulation of survivin. Clin Cancer Res 2017;23:4301–11. [PubMed: 28314790]

Significance: These findings provide evidence that inhibitors of NF-κB signaling synergize with BET inhibition in *in vitro* and *in vivo* models, suggesting a clinical utility of these targeted therapies in patients with uveal melanoma.

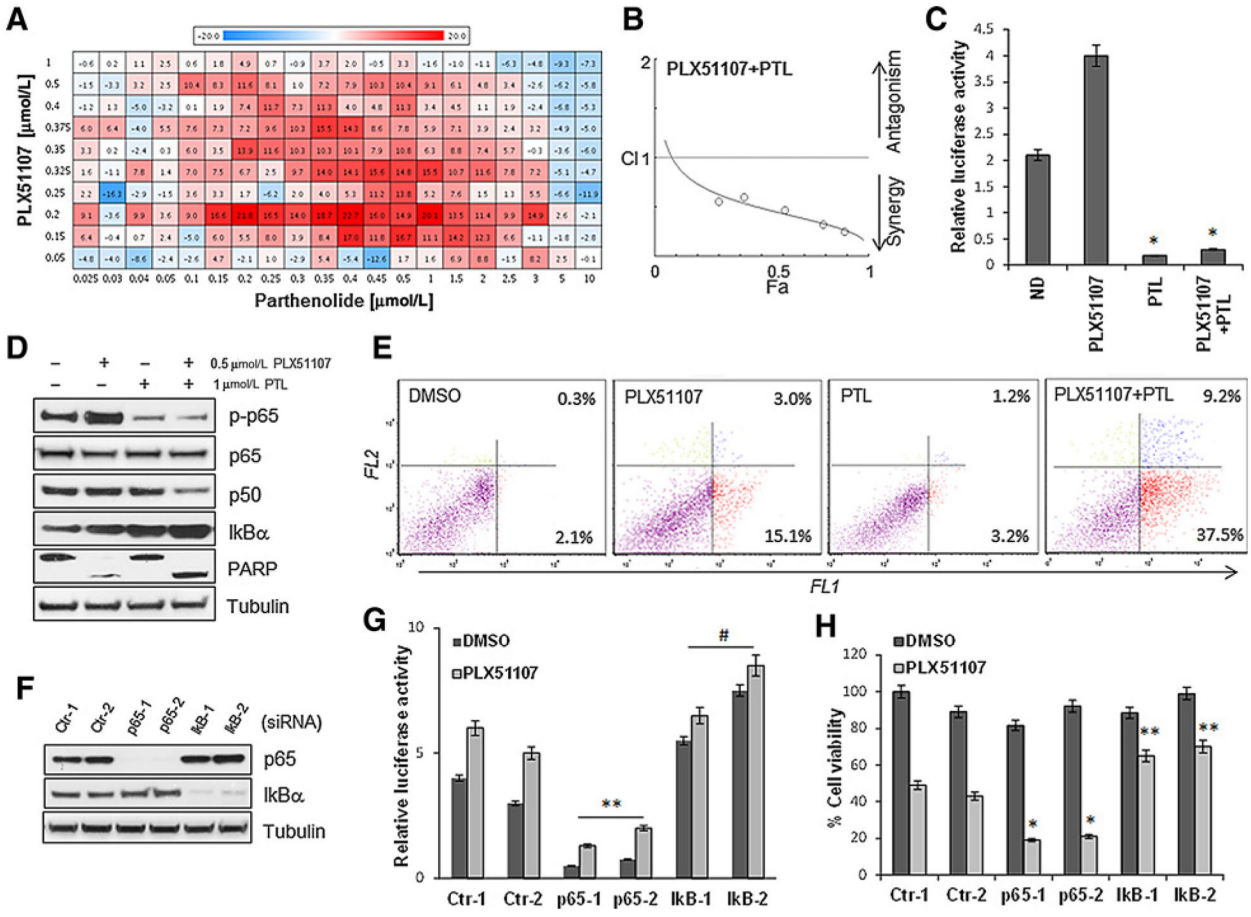

Figure 1.

Parthenolide has synergistic activity in combination with PLX51107 in a high-throughput drug screening. **A**, Uveal melanoma cells (92.1) were treated in secondary screenings with increasing concentrations of PLX51107 (0.05–1 µmmol/L) and parthenolide (0.025–10 µmmol/L) for 72 hours. The Bliss values for positive interactions (additive/synergy) are indicated in red and negative interactions in blue. **B**, Chou–Talalay plot (x-axis, Fa, or fractional activity, reflects the fraction of cells affected by the drug treatment relative to vehicle controls; y-axis, combination index, with <1, >1, and = 1 indicating synergistic, antagonistic, and additive effects, respectively). Each point represents a different combination of drug concentrations. **C**, The cells were transfected with a vector containing an NF-κB reporter gene along with a Renilla luciferase vector (1:10 ratio), then treated with 0.5 µmmol/L PLX51107, 1 µmmol/L PTL, and the combination for 24 hours. Luciferase activity was determined by chemiluminescence. Results are normalized to Renilla luciferase activity and represent the mean ± SD.*, $P < 0.005$.**D**, Western blot analysis of 92.1 cells treated with 0.5 µmmol/L PLX51107 and 1 µmmol/L PTL alone and in combination for 48 hours, showing inhibition of p65 phosphorylation, decreased expression of p50, induction of IkBα, and PARP cleavage. **E**, Apoptosis assay of 92.1 cells treated with 0.5 µmmol/L PLX51107 and 1 µmmol/L PTL alone and in combination for 48 hours, measuring cell permeability to fluorescent stains YO-PRO (FL1, for early apoptosis) and propidium iodide (FL2, for late apoptosis). **F**, Immunoblotting of cells transfected with two control (siCtr-1,

−2), two p65 (sip65–1, −2), and two IkBα (IkB-1, −2) siRNA. **G**, The siRNA-transfected cells were then transfected with the NF-κB reporter gene vector/*Renilla* and tested for luciferase activity.**, P < 0.01; #, P < 0.05, comparing sip65–1,−2 with control siRNA. **H**, Cell viability assays of cells depleted of the indicated proteins after treatment with PLX51107 for 72 hours. Bars, mean ± SD.*, P < 0.005; **, P < 0.01.

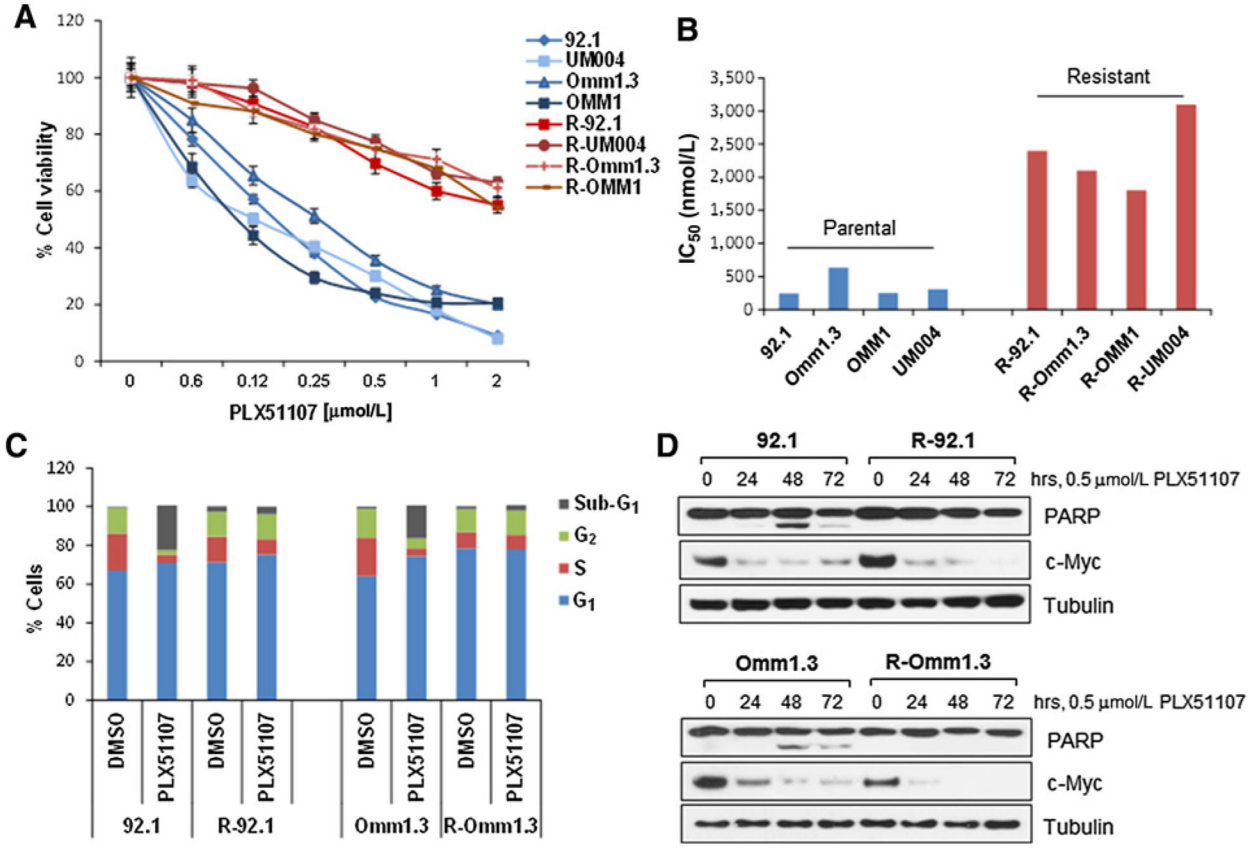

Figure 2.

Uveal melanoma cells develop resistance to BET inhibitors. **A**, Proliferation assays of uveal melanoma cell lines 92.1, Omm1.3, UM004, OMM1 (blue), and their resistant counterpart R-92.1, R-Omm1.3, R-UM004, R-OMM1 (red). Cell viability after 72 hours was calculated as percentage of untreated controls. Each point is a mean ± SD. **B**, The IC_{50}s were calculated using the CompuSync software. The parental cell lines showed IC_{50} = 200–600 nmol/L, while for the resistant cells IC_{50} = 1,600–2,500 nmol/L. **C**, Parental and BETi-resistant cells were treated with DMSO or 0.5 µmmol/L PLX51107 for 48 hours, then stained with propidium iodide and analyzed for cell-cycle distribution by flow cytometry. The sub-G_1 population was 23% for 92.1 and 17% for Omm1.3, while R-92.1 and R-Omm1.3 cells showed 4% and 3%, respectively. **D**, 92.1 and Omm1.3 cells were treated with 0.5 µmmol/L PLX51107 for up to 72 hours, and cell lysates were analyzed by immunoblotting for expression of c-Myc, PARP, and tubulin.

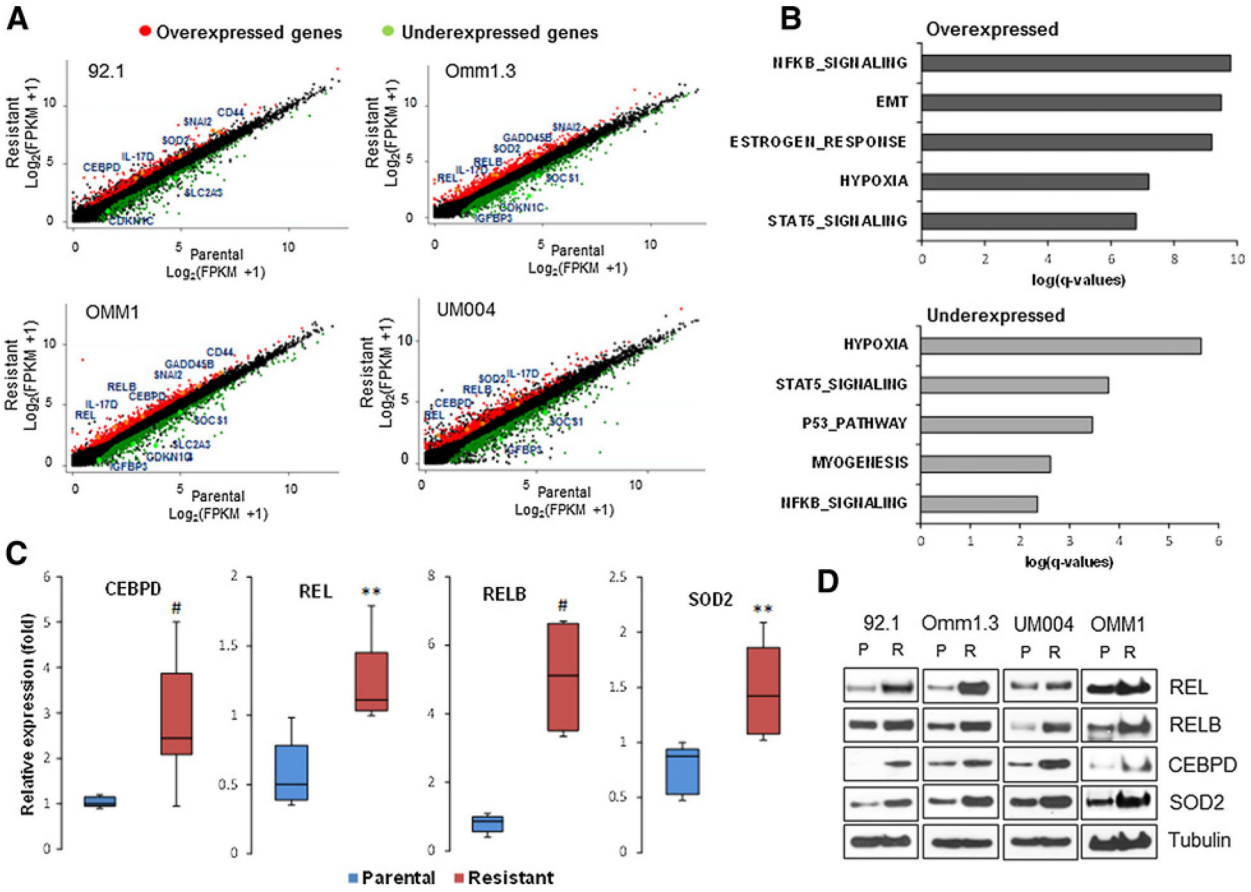

Figure 3.

RNA sequencing and GSEA. **A**, Scatter plots of candidate genes in the given cell line showing overexpression (red) and underexpression (green) in at least two cell lines. Selected genes with high differential expression are indicated. **B**, GSEA for differentially over- and underexpressed genes in the resistant cells at baseline. The bars show the log(*P* value) from a Fisher exact test for enrichment for each pathway. **C**, Validation of gene expression by qPCR analysis using gene-specific primers for CEBPD, REL, RELB, and SOD2 in all four parental and four BETi-resistant cell lines. Triplicate values were normalized with GAPDH using the $\Delta\Delta C_t$ method and reported as distributions of fold change relative to untreated 92.1 cells (set at 1) between the two groups (parental and resistant cells).#, $P < 0.05$; **, $P < 0.01$. **D**, Immunoblotting of parental and BETi-resistant cells using antibodies for the indicated proteins. Each blot is representative of at least two experiments showing same results.

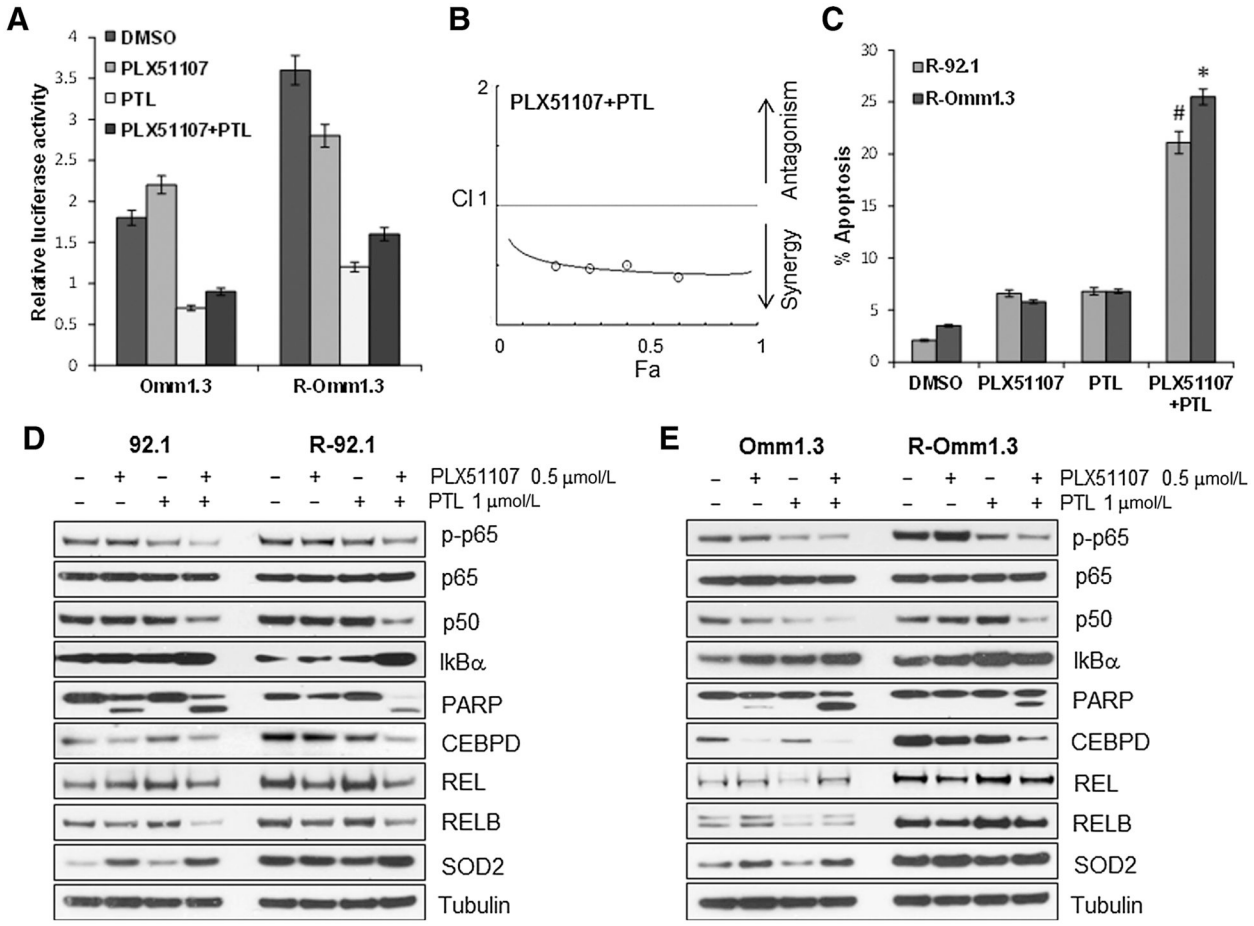

Figure 4.

Inhibition of NF-κB restores sensitivity to PLX51107 in BETi-resistant cells. **A**, NF-κB luciferase reporter gene assay of parental and resistant cells after treatment with PLX51107 (0.5 μmmol/L), PTL (1 μmmol/L), and the combination for 24 hours. **B**, The combination PLX55107 + PTL is synergistic (CI < 1). Each point represents a different combination of drug concentrations. **C**, Quantification of apoptotic cells for the experiments shown inþSupplementary Fig. S7. #, $P < 0.05$;*, $P < 0.001$.**D** and **E**, Parental and resistant 92.1 and Omm1.3 cells were analyzed by immunoblotting for the indicated proteins after 48-hour treatments with 0.5 μmmol/L PLX51107, 1 μmmol/L PTL, and the combination. The concurrent inhibition of BET and NF-κB reduces the expression of p-p65, p50, and CEBPD, while inducing PARP cleavage.

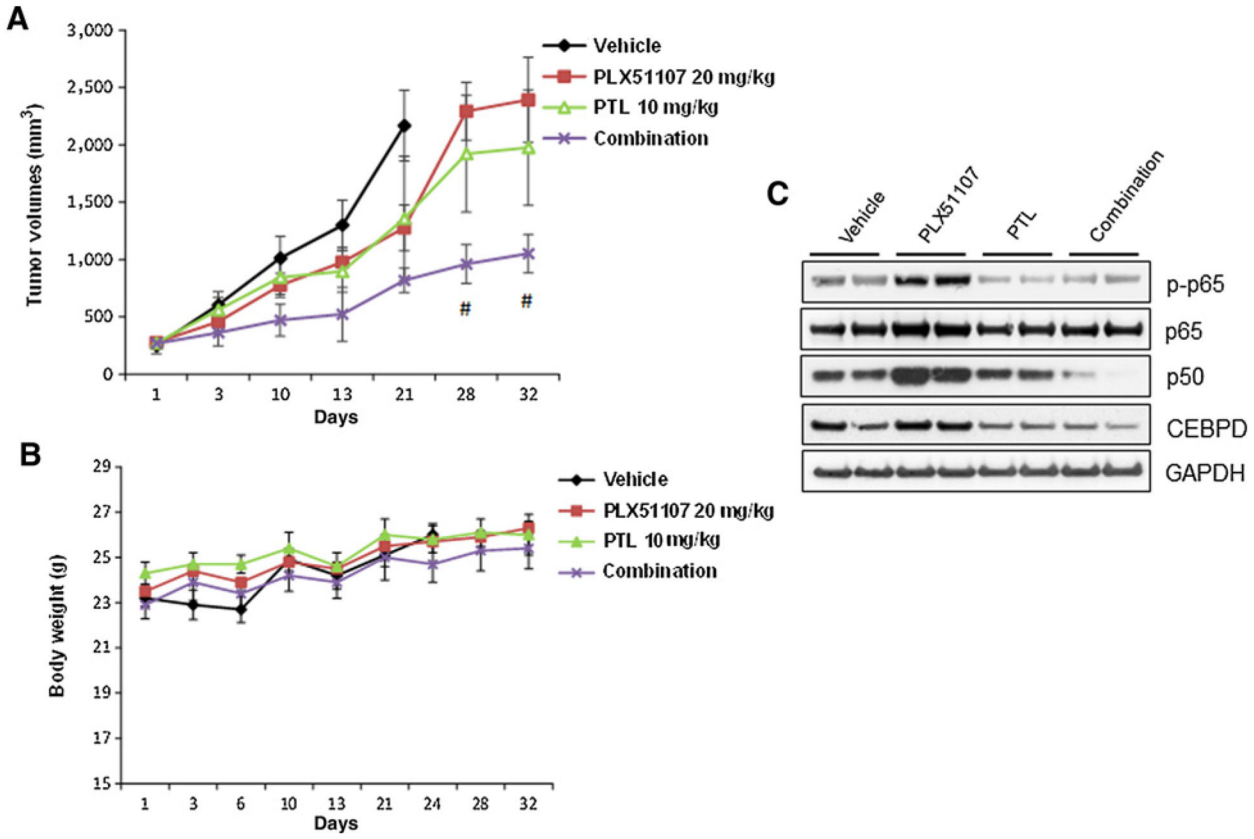

Figure 5.

Inhibition of NF-κB increases sensitivity to BET inhibition *in vivo*. **A**, Tumors derived from R-Omm1.3 cells were implanted in athymic nu/nu mice. When these tumors reached an average of 270 mm^3 diameter, the mice were administered (7/group) with vehicle or PLX51107 20 mg/kg orally, PTL 10 mg/kg i.p., and the combination of the two drugs. The treatment duration was 3 weeks for vehicle and 5 weeks for the drug treatments. The tumor size was measured twice a week. Each value represents the mean measurement of at least 5 animals. ± SEM, #, $P < 0.05$. **B**, Body weight of the host mice was measured twice a week. **C**, Two xenograft tumors per group were lysed at the end of the treatments and analyzed by Western blotting with the indicated antibodies.

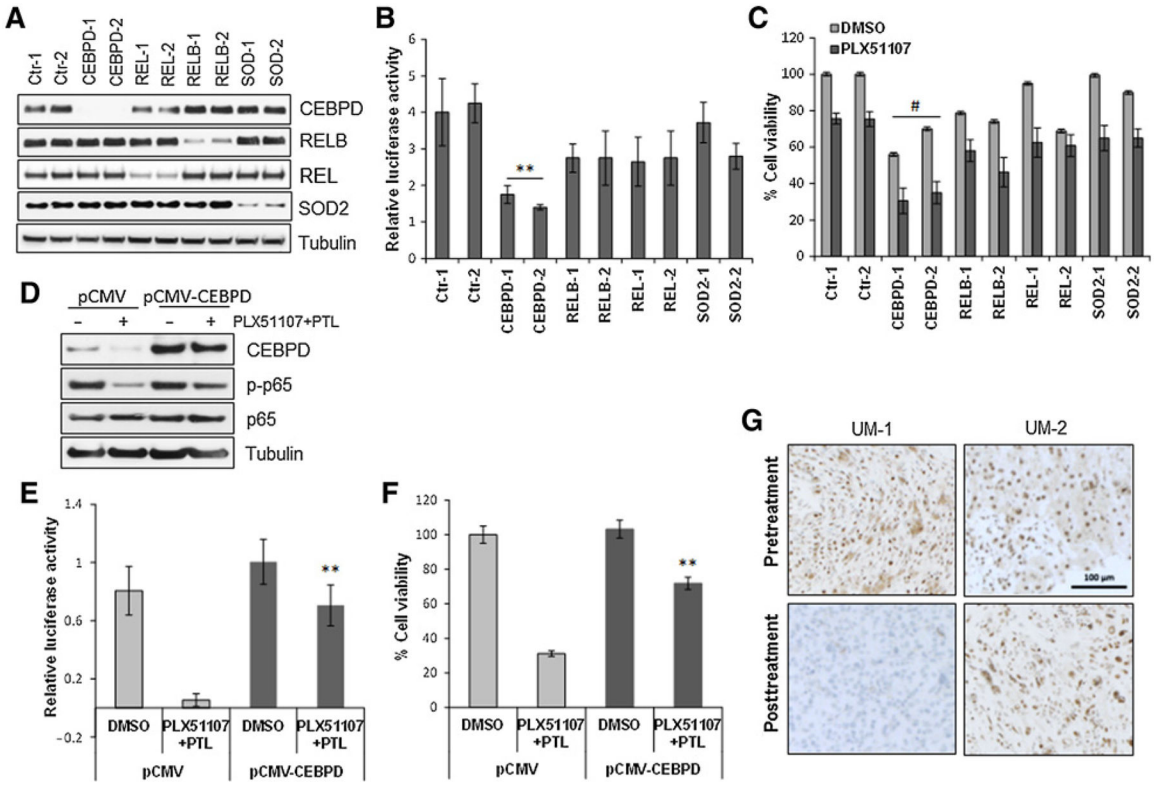

Figure 6.

Effects of gene silencing in the resistant phenotype. **A**, The indicated genes were silenced with two independent siRNA in the cell line R-92.1. Two nonspecific siRNAs were used as controls. **B**, siRNA-depleted cells were than transfected with an NF-κB-Luc vector and tested for NF-κB activity.**, $P < 0.01$. **C**, Cell viability assay of siRNA-transfected cells in the presence of 0.5 μmmol/L PLX51107 after 72 hours. Bars, mean ± SD. #, $P < 0.05$. **D**, R-92.1 cells were transfected with an empty vector (pCMV) or a CEBPD construct (pCMV-CEBPD). Cell lysates were subjected to immunoblotting using antibodies for CEBPD, p-p65, p65, and tubulin. **E**, NF-κB-Luc activity in vector and CEBPD-expressing cells with or without the combination treatment PLX51107 + PTL. **, $P < 0.01$. **F**, Viability assay of CEBPD-transfected cells after the combination treatment for 72 hours. Columns, mean ± SD of three independent experiments. **, $P < 0.01$. **G**, IHC analysis of CEBPD expression at baseline and after 2 weeks of treatment with PLX51107 in specimens from two representative patients with uveal melanoma. Suppression of CEBPD staining was observed after treatment in patient UM-1 who achieved prolonged stable disease lasting more than 1 year. Patient UM-2 had no significant changes in CEBPD expression and experienced disease progression.